Light Metals 2011 *Edited by: Stephen J. Lindsay*
TMS (The Minerals, Metals & Materials Society), 2011

ANODIC VOLTAGE OSCILLATIONS IN HALL-HÉROULT CELLS

Kristian Etienne Einarsrud[1] and Espen Sandnes[2]

[1]Department of Energy and Process Engineering, Norwegian University of Science and Technology, N-7491 Trondheim, Norway. [2]Hydro Aluminium AS, Primary Metal Technology, N-6882 Øvre Årdal, Norway

Keywords: Anodic gas bubbles, lab scale measurements, industrial scale measurements, optical methods

Abstract

Experiments on lab- and industrial scale cells have been conducted in order to study the behaviour of anodic gas bubbles under various operating conditions. Traditional voltage measurements have been supplied with high-speed video recordings of the bath surface showing a good correspondence between voltage fluctuations and escaping gas bubbles. On average, 0.5 and 2 bubbles were observed per second in each respective case. Average frequencies obtained by a FFT of the voltage signal however show significantly lower values, approximately half of that observed. It is shown that this discrepancy can be due to large variations in the bubble release times. Observed bubble events can be related to FFT frequencies by means of a frequency based on statistically significant periods. For industrial anodes, the possibility of overlapping bubbles is investigated as alternative effect resulting in the mismatch between observed and calculated frequencies.

Introduction

As stated in the introduction of the recent review by Cooksey et al. [1], "the contribution of gas bubbles to electrical resistance in aluminium reduction cells is becoming increasingly important as smelters attempt to reduce energy consumption". The importance of anodic gas bubbles arises from their negligible conductivity, effectively screening out sections of an operating anode.

In practical models the influence of the gaseous bubbles is often treated as a gas coverage factor θ and a gas layer thickness d_b and a review of the various models used for determining d_b and θ is found in Hyde and Welch [2]. For typical operational values, the bubbles can be responsible for as much as 10% of the voltage drop, which is a pure *loss* of energy through Ohmic heating.

The Hall-Héroult cell has a strong dynamic nature due to buoyant bubbles and strong MHD coupling. Hence, it should come as no surprise that the anodic voltage varies with time. There are several sources to these variations, ranging from high frequency ripples in the DC current applied to the cell, to low frequency MHD-instabilities creating large scale wave motion of the metal pad. A special frequency band ranging from 0.5 to 5 Hz has been credited to bubbles and the produced signal denoted as bubble noise (cf. for instance Wang and Tabereaux [3] and Kalgraf et al. [4] and references therein.).

The relation between gas coverage fraction and bubble noise has recently been treated by Kiss [5] in a numerical model, showing that the nature of the bubble noise is highly dependent on the number of bubbles present beneath the anode. A regular pattern in θ is observed for single bubbles, corresponding to its regular growth and departure. When many bubbles are present, the combined effect of growing, coalescing and detaching bubbles results in random like fluctuations. However, under certain conditions, bubbles can manifest a concerted movement due to very big gas pockets sweeping longside the anode, engulfing lesser bubbles in its motion, yielding a so called quasi periodic self organized motion of bubbles and hence variation in the cell voltage.

Although periodic behaviour has been observed by several authors (cf. Wang and Tabereaux [3], Wang et al. [6] and Xue and Øye [7]), results appear to depend significantly upon electrolysis parameters as well as the geometry of the anode. The last point is somewhat alarming as the results in the references above are all obtained on small lab-scale anodes which not necessarily produce the same physics as that encountered on industrial scale. Actually, Wang and Tabereaux [3] even point out that no direct studies have been reported regarding the bubbling phenomena occurring in commercial cells. Hence, even though it is crucial for validation purposes, the relation between lab- and industrial scale anodes appears to have been given little focus.

A complete treatise on the relation between lab- and industrial scales is, necessarily, beyond the scope of the present work. Instead, the main focus will be to study the most significant properties of anodic gas bubbles and determine whether or not it is meaningful to transfer observations made on lab scale to an industrial setting.

Experimental setup

In order to see the relation between industrial- and lab scale measurements, both settings have been investigated. Industrial measurements were conducted at Hydro Reference Center in Årdal, October 2009, while lab scale measurements on a moderate sized anode were conducted at SINTEF Materials and Chemistry in Trondheim, March 2010. On both scales, two parallel sets of observations were conducted; high frequency measurements of anodic voltage and high frequency *observations* of escaping gas bubbles. In essence, the high frequency observations are video recordings of the (upper) bath interface taken at such high sampling rates that the interface movement due to *individual* escaping bubbles could be observed. A sketch of the experimental setup is shown in figure 1.

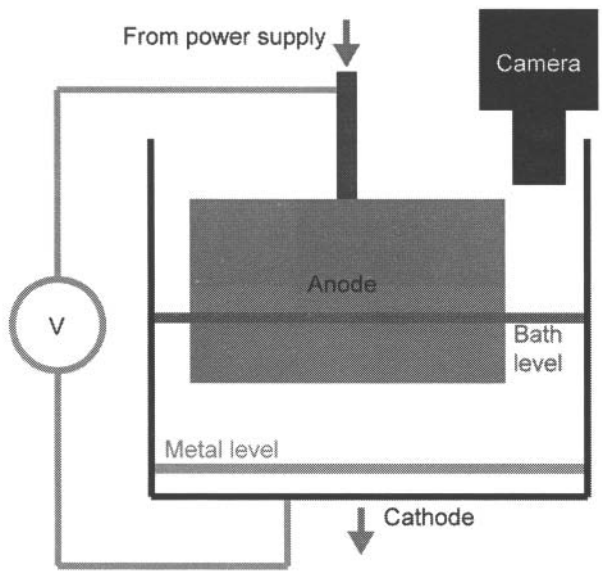

Figure 1: Simplified sketch of experimental setup.

For practical reasons, the camera could not be placed directly above the bath surface in the industrial setting. Instead, the bath surface was recorded through a tap hole at the end of the cell. This necessarily restricts observations to the bath interface between the two end anodes. This is however not believed to significantly influence the bubble noise, as confirmed from measurements on anodes not situated at the end.

The cell voltage was logged at 50 Hz using a CR23X multilogger from Campbell Scientific with resolution 1.6 μV and an accuracy of 25μV for lab scale experiments, while the frequency was 10 Hz on industrial scale. The motion of the bath interface due to escaping bubbles was recorded using a PHOTRON 1024PCI FASTCAM digital camera, controlled by a laptop PC by means of a PCI bus, at 250 fps. The camera was supplied with a Nikon 28-85 mm zoom-lens and was mounted on a tripod.

The industrial cell operated at approximately 315kA under standard electrolysis condtitions, while the lab scale experiments were set up as follows: A 100 by 100 mm anode was made from industrial carbon and placed in a cylindrical graphite lined crucible lined with Si_3N_4-SiC with inner diameter 220 mm. The anode was fixed to a steel rod so that the anode-cathode distance could be varied. The anode was connected to a power supply (type LAMBDA ESS) allowing for currents up to 500 A. The experiments described in the following where conducted at up to 110 A yielding current densities of 1.22 A/cm^2. Initially, 6.7 kg of bath (aiming at 11wt% excess AlF_3, 5wt% CaF_2 and 4wt% Al_2O_3) was melted and standard industrial alumina was added at regular intervals.

Eight lab scale and three industrial scale experiments were conducted. Lab scale experiments are summarized in table I.

Table I: Summary of lab scale experiments

Experiment (#)	Amperage (A)	ACD (mm)	Temperature °C
1	80	40	975
2	80	40	975
3	110	15	969
4	80	40	969
5	110	40	970
6	110	15	966
7	80	40	966
8	80	15	966

Data from the voltage measurements was filtered before a statistical and spectral (FFT) analysis was performed using MATLAB. Due to bad contrast, video recordings were analyzed manually in order to obtain data for comparison.

Results

Identification of bubbles

As noted in the previous section, industrial scale recordings were performed through an (enlarged) tap hole at the

end of the cell. As a consequence, *all* bubbles escaping from either of the two anodes adjacent to the hole in question. Fortunately, large gas bubbles typically accumulate a large portion of momentum during their travel beneath the anode, a motion which is continued even after release at the anode edge (cf. Einarsrud [8] for details), resulting in right or left-bound bubbles on the bath-surface, depending upon the anode of origin. Bubbles originating from different (industrial) anodes are shown in figure 2.

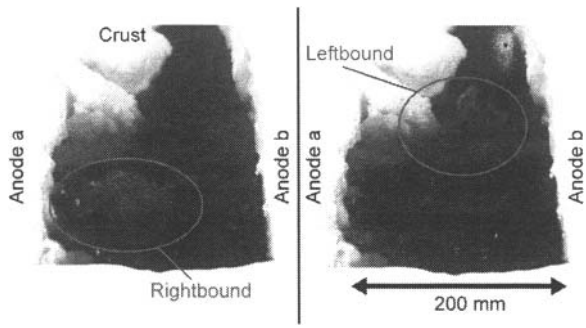

Figure 2: Distinction between bubbles originating from different anodes (denoted a and b) from escape direction. Left-bound bubble originates from anode b while right-bound bubble originates from anode a. View is approximately at 45° with horizontal.

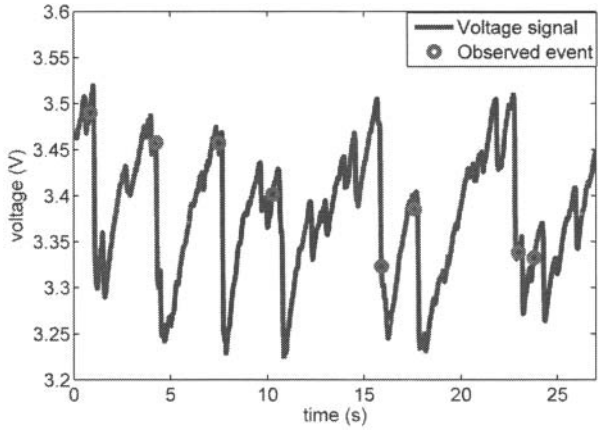

Figure 3: Measured voltage signal (solid line) and observed bubble events (circles) for lab scale experiment #2.

Relation between signal and observation

As video recordings and measurements were started simultaneously, the time of an observed event can be compared directly to the measured time series. Such a comparison is shown in figure 3.

As seen from figure 3, the sharp decrease in the measured voltage corresponds very well to events related to detaching and escaping bubbles, as for micro-anodes such as the one used by Xue and Øye [7]. Lab-scale observed events account for approximately 95% of the fluctuations with amplitude larger than 3% of the average voltage, suggesting a close relationship between small and moderate size anodes.

Significant properties of bubble noise

The average observed bubble frequency $\bar{f}_{OB}$ is simply defined as

$$f_{OB} = \frac{N_{OB}}{T_O}, \tag{1}$$

where N_{OB} is the number of observed bubbles over the observation time T_O, which is equal to 25.6 seconds. Given a *periodic* sequence of events, the observed bubble frequency should be close to the most dominant frequency, f_1 obtained from a FFT of the corresponding signal. Most and second most dominant FFT frequencies, f_1 and f_2, observed frequencies, f_{OB}, as well as (average) relative magnitude of voltage oscillations, $\bar{A}_{\%}$ are given in table II.

As seen from table II, high frequencies appear to be related to *small* amplitudes in voltage oscillations. As noted by Kiss [5], high frequency regimes are related to small amplitudes in the bubble coverage factor θ, resulting in smaller voltage fluctuations. The same tendency is observed by Wang and Tabereaux [3], postulating inverse proportionality between the magnitude of the fluctuation and bubble frequency.

The relative magnitude of the oscillations as well as typical frequencies fit well within the values expected for bubble noise. Table II shows that observed frequencies are *significantly* higher that those obtained from the FFT of the corresponding signal; almost four times higher in the extreme case of experiment I2a.

Interpretation of frequency

The apparent discrepancy between observed and FFT-frequencies can be due to the *lack* of periodicity in the bubble noise signal from moderate and industrial size anodes. The *average* escape time for each set of experiment

is 1.99 and 0.51 s for each respective case, suggesting frequencies of approximately 0.5 and 2 Hz, which is close to the values expected. The corresponding standard deviation is (on average) found to be 0.99 s on lab- and 0.35 s on industrial scale. This is a significant variation suggesting that the assumption of a periodic signal does not hold, making a meaningful spectral analysis of the signal challenging.

Table II: Comparison of frequencies in bubble noise for lab- (#) and industrial (I#) measurements.

Exp. (#)	$A_{\%}$ (%)	f_{OB} (Hz)	f_1 (Hz)	f_2 (Hz)	f_{ss}^T (Hz)
1	5	0.36	0.20	0.29	0.25
2	6	0.31	0.15	0.34	0.17
3	4	0.38	0.39	0.34	0.31
4	3	0.36	0.22	0.17	0.25
5	5	0.47	0.24	0.56	0.35
6	2	0.85	0.71	0.56	0.71
7	2	0.66	0.37	0.24	0.37
8	2	0.61	0.55	0.45	0.50
I1	3	1.88	0.76	0.86	1.32
I2a	4	1.95	0.55	0.32	1.45
I2b	2	1.95	0.88	0.55	1.33

The interpretation of frequency used to compute f_{OB} should strictly only be considered as an average property and a one to one correspondence to the FFT frequency is expected only if the signal is purely periodic. Evidently, this is not the case for the signals obtained in the present work. In order to capture the variations in bubble release time, the frequency of statistically significant events is computed as

$$f_{ss}^i = \frac{N_{ss}}{T_O}, \tag{2}$$

where T_O is the observation time and N_{ss} is the number of statistically significant events. An event is denoted as statistically significant if its value is in the range $\mu \pm \sigma$, where μ is the mean value and σ is the standard deviation of the dataset in which the event in question occurs. The range is chosen so that at least 50% of the events in the dataset are included (given that the dataset follows a normal distribution). Frequencies obtained from the number of significant bubble periods (f_{ss}^T) are shown in table II. As seen from table II, frequencies based on statistically significant events reproduce the calculated FFT frequencies with an average absolute error of less than 20% for lab-scale measurements. Although somewhat improved, frequencies from industrial scale measurements still compare poorly.

Large scale effects

As noted by Kiss and Poncsak [9], the frequencies of individual bubbles are very difficult to observe. Besides the influence from their release at the anode edge, interactions between moving bubbles and their coalescence dominate the spectrum of the voltage fluctuations, i.e. it is the collective bubble behaviour under the anode which is measured as a voltage signal.

Based on this a hypothetical collective bubble signal is reconstructed based on the observed release frequencies. The procedure used is as follows:

- The time from which a bubble appears on the surface to the time it escapes is registered.
- The bubble escape time, combined with the extent of the splashing gives an indication of the bubble size, which is divided into three classes (0.25, 0.5 and 1).
- The residence time under the anode is approximated from the bubble escape time.
- Based on the approximated residence time and the size class, a resistance-curve is obtained for each individual bubble.
- The total signal is computed from the sum of each individual bubble.

Figure 4 shows the time of escape for bubbles originating from experiment I2a. The magnitude of each peak is determined from the size of the corresponding bubble.

As expected, the time of escape is irregular, bubbles appearing as bursts rather than at a distinct frequency. Furthermore, several of the peaks are separated by very small time intervals, close to the sampling time used in the voltage measurements. This overlap becomes even more visible when a linear relation between the first appearance of the bubble and its time of escape is plotted (assuming the appearance of the bubble has zero magnitude), as in figure 5. As noted by Kiss and Poncsak [9] and observed in water models and simulations (cf. Einarsrud [8]), the nature of the bubble changes dramatically when detaching at the anode edge; from an elongated flat bubble under the anode to a more spherical shape in the center channel. As a consequence, the residence time of the bubble is greater under the anode, compared to its residence time in the center channel (i.e. the time from its appearance to its escape).

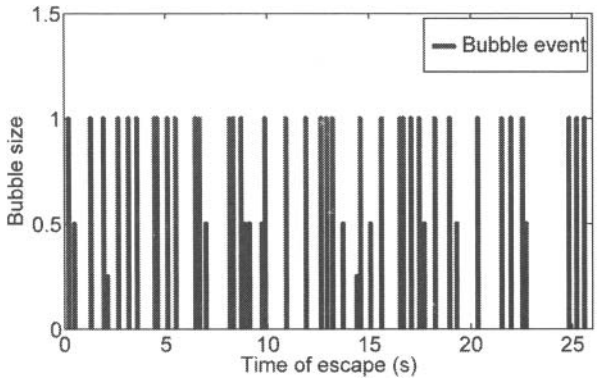

Figure 4: Escape time and estimated bubbles size from experiment I2a.

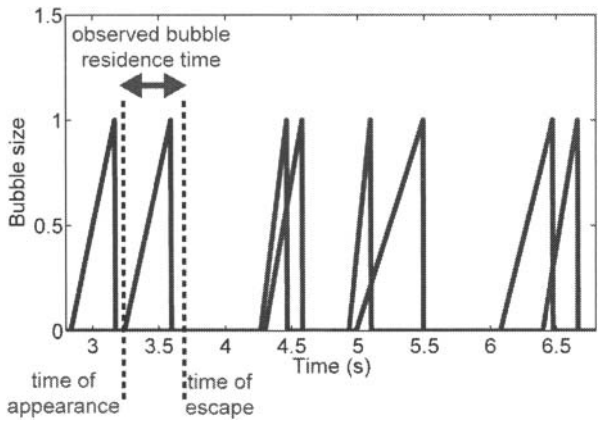

Figure 5: Linear bubble growth from time of bubble appearance to escape for experiment I2a.

The bubble residence time for an equivalent volume bubble under the anode can be approximated by the simple relation

$$t_{anode} = t_{channel} \frac{\bar{U}_{channel}}{\bar{U}_{anode}} \frac{L_{anode}}{L_{channel}}, \quad (3)$$

where $\bar{U}_{channel}$ and $\bar{U}_{anode}$ represent average bubble velocities in the channel and under the anode and L_{anode} and $L_{channel}$ represent typical lengths travelled by a bubble. The velocity in the channel is greater than under the anode, though the magnitude is the same (cf. Einarsrud [8]). The length scales are however significantly different; the typical anode length being of order 100 cm, while the typical bath height is 20 cm. Hence, the approximated bubble residence time under the anode is

$$t_{anode} \approx 5 t_{channel}, \quad (4)$$

yielding the bubble growth curve shown in figure 6.

Comparing figures 5 and 6, it is clear individual bubbles in principle can overlap if the anode is of large size. A hypothetical bubble signal is constructed by adding the contribution of each individual bubbles shown in the above figure. Performing a FFT on this signal results in dominating frequencies in the range of 0.3 to 0.70 Hz, which is remarkably close to the measured values (cf. table II).

The most critical parameter in the above analysis is the approximation of the bubble residence time. Changing the value of the pre factor from 5.0 to 2.5 increases the maximum frequency from 0.49 to 0.64 Hz, while a value of 1.0 yields a frequency of 1.1 Hz. It is thus clear that the bubble residence time has a large impact on the resulting spectrum; lower residence times yielding higher frequencies. Recalling how the bubble residence time is defined (equation 3), a reduced residence time is equivalent to a shortening of the anode in the bubble flow direction.

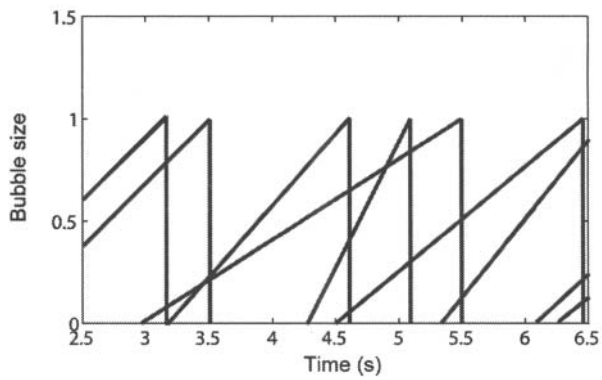

Figure 6: Linear bubble growth from approximated bubble residence time under anode for experiment I2a.

A similar increase in dominating frequencies is predicted by Kiss [5], showing an increase in frequency of a factor close to two when the aspect ratio of the anode is changed correspondingly, *for a given flow regime.*

The final point is important as the flow regime necessarily depends upon the anode geometry, as the present lab scale (and hence smaller length) experiments show a tendency towards *lower* frequencies than their (larger) industrial counterparts. A dependency upon anode size is also found by Wang et al. [6], suggesting the possibility of an optimum anode size for a given current density.

Concluding remarks

Voltage measurements combined with visual observations show that anodic bubbles are responsible for a distinct class of voltage fluctuations on both lab- and industrial scale. In both cases, anodic bubbles yield voltage fluctuations with average frequencies in the range of 0.5 to 2 Hz and amplitudes as large as 10% of the mean voltage. In the cases studied higher frequencies were in general found on industrial scale.

Although the present results appear to, on average, have properties similar to those obtained in small scale lab investigations, a detailed analysis reveals that large variations in bubble release times are present; bubbles releasing in seemingly random bursts rather than at regular periodic times. These phenomena are believed to be coupled to anode size and geometry, which in turn influence the bubble flow regime. For a given flow regime, the bubble residence time under the anode has a large influence on the resulting spectrum, indicating that the low-frequency oscillations observed in industrial Hall-Héroult cells are due to the *collective* behaviour of several large anodic bubbles. This finding suggests that measurements on small lab scale anodes not necessarily represents the reality encountered on large scale industrial anodes. Small scale measurements could however be used to validate the *local* behaviour on an industrial anode.

Throughout this work (and in the overall literature) the term "frequency" has been used to describe anodic bubble noise. Results presented herein however indicate that typical signals are not strictly periodic, hence violating the basic assumption of the traditional FFT analysis. This suggests that a frequency based description not necessarily is the best way of treating bubble noise and a more general framework is needed to describe bubble noise in industrial processes. This will however be the topic of future research.

Acknowledgements

The present work was financed by Hydro Aluminium, Primary Metal Technology with support from the Research Council of Norway. Permission to publish the results is gratefully acknowledged. The authors would like to thank SINTEF Materials and Chemistry and Hydro Aluminium for inclusion in their ongoing experiments and for all valuable help with equipment and experimental setup. Also, all suggestions and recommandations given by Stein Tore Johansen, Asbjørn Solheim, Egil Skybakmoen, Iver H. Brevik and Eirik Manger are greatly acknowledged.

References

[1] Cooksey M. A., Taylor M. P. and Chen J. J. J., Resistance Due to Gas Bubbles in Aluminium Reduction Cells. Journal of Metals February 2008, 51-57.

[2] Hyde T. M. and Welch B. J., The Gas under Anodes in Aluminium Smelting Cells Part I: Measuring and Modeling Bubble Resistance under Horizontally Oriented Electrodes. Light Metals 1997, 333-340.

[3] Wang X. and Tabereaux A. T., Anodic Phenomena - observations of anode overvoltage and gas bubbling during aluminium electrolysis. Light Metals 2000, 1-9.

[4] Kalgraf K., Jensen M. and Pedersen T. B., Theory of bubble noise, bath height and anode quality. Light Metals 2007, 357-361.

[5] Kiss L. I., Transport processes and bubble driven flow in the Hall-Héroult cell. 5th Int. Conf. on CFD in Proc. Ind., CSIRO, Melbourne, Australia, 2006, 1-7.

[6] Wang Z., Gao B., Li H., Shi Z., Lu X. and Qiu Z., Study on Bubble Behavior on Anode in Aluminium Electrolysis - Part I. Light Metals 2006, 463-466.

[7] Xue J. and Øye H. A., Bubble behaviour - Cell voltage oscillation during aluminium electrolysis and the effects of sound and ultrasound. Light Metals 1995, 265-271.

[8] Einarsrud K. E., The Effect of Detaching Bubbles on Aluminum-Cryolite Interfaces: An Experimental and Numerical Investigation. Metallurgical and Materials Transactions B, Vol. 41:3, 2010, 560-573.

[9] Kiss L. I. and Poncsak S., Effect of the bubble growth mechanism on the spectrum of voltage fluctuations in the reduction cell. Light Metals 2002, 217-223.